

Proceedings of the ASME 2022 Conference on Smart Materials,
Adaptive Structures and Intelligent Systems
SMASIS2022
September 12-14, 2022, Dearborn, MI

# SMASIS2022-91047

# DEVELOPMENT OF EMBEDDABLE ADDITIVE MANUFACTURING MICROSENSORS FOR STRUCTURAL HEALTH MONITORING

# Nicholas Reed, Daewon Kim

Embry-Riddle Aeronautical University, Daytona Beach, FL

## **ABSTRACT**

Significant progress into the development and use of stretchable sensors for structural health monitoring (SHM) has been made in the last several years. The fusion of stretchable, adaptable sensing materials with highly specialized additive manufacturing techniques allows for the development of highly adaptive, customizable, and easily accessible sensing solutions. However, a significant portion of these works explore SHM topics at a macro level, and with a reduced focus on implementation. As such, little application or experimentation into practical sensing elements, especially those at the micro scale, have followed the advances in sensing technology. In this work, we demonstrate the application of recent developments in stretchable electronics, alongside multiple advanced additive manufacturing processes, to develop a novel flexible microscale sensor. A complex sensor is designed and printed utilizing Digital Light Processing (DLP) to directly fabricate the structure. The printed sensor is then filled with a piezoresistive sensing element of either PEDOT:PSS or carbon-based PDMS (cPDMS), which provided strain readings via resistance change. After being filled with a sensing mixture, the sensor is shown to operate as desired under large deformations. Additionally, the sensor is shown to work effectively when embedded into a separate additively manufactured part. A flexible test coupon is manufactured using the DLP AM process, and a microsensor is embedded inside the coupon structure. This sensing systems is tested in both tension and bending. These results show the feasibility of implementing both modern day AM processes and into current structural health monitoring developments into practical applications.

Keywords: Structural Health Monitoring, Additive Manufacturing, Sensing

### 1. INTRODUCTION

The development and implementation of stretchable electronics for use in sensing technologies has been a research field of significant focus for aerospace applications [1-5]. Recently, the investigation into sensing technologies has exploded in scope, with significant progress in a large variety of

sensor classes, such as mechanical [6-11], electrical [12], optical [13], and chemical [14] sensors. Specifically, piezoelectric sensors have benefitted from the advances in material science, allowing for complex polymers that feature a wide variety of favorable characteristics for sensor technologies, such as adjustable and favorable rheological properties, self-healing capabilities [15], tunable sensing parameters [16-17], and ease of manufacture [6,10,18]. These advances are compounded upon with the proliferation of additive manufacturing techniques as a primary means of fabricating whole sensors or critical subsections of sensors. Since AM techniques offer the capacity to rapidly prototype and enhance a wide variety of designs with complex features at high speeds, research can quickly iterate on successful avenues of investigation. These intersecting contributions have greatly enhanced the breadth of sensing technologies and improvements.

However, with an increased focus on exploring these new sensing technologies, implementations and adaptations are often lacking in depth and refinement. Typically, a sensor is tested at a macro- to meso-scale, with an incredibly simple geometry being manufactured with an AM process, and often left without further refinements to the design. This regiment of testing confirms the validity of the sensing technology as a whole, but does not yield much insight into the implementation of the researched technology into practical sensing applications; most sensors are not meso-scale lines that are applied at a surface level [2,4,7,8,12-13,21]. In addition, research into applications of sensing technology for micro-scale applications is sparse compared to other larger scales [1-3,6-8,11,18,21].

Integration of sensing systems adds another layer of complexity to the creation and development of successful new sensing technologies. Encasing a raw sensing element into a suitable substrate can be a challenging task in of itself, especially in aerospace applications where substrate choices are highly limited. Often times, AM processes are used to develop onto or into molded or otherwise unworked easy to use polymers, such as PDMS [7-8,12,16]. However, application of these completed sensors into practical elements, such as specimens usable in tensile or flexural testing, is often overlooked.

This paper presents the integration and application of both cPDMS and PEDOT:PSS:TritonX piezoresistive sensing mixtures into a practical overall sensing element: a flexible test coupon, capable of application to a wide variety of aerostructures. The sensor utilizes AM processes in fabricating the sensing element, the sensor housing, and the application test coupon. After manufacture, the test coupon is subjected to loading conditions, and the performance of the sensor is compared to theoretical and simpler sensing element validation testing common in literature. Additionally, the structure of the fully embedded dogbone is examined to ensure proper and complete integration of the sensor into the tested sample.

#### 2. MATERIALS AND METHODS

This section describes the sensor fabrication procedures, manufacturing properties and experimental analysis.

# 2.1 Materials and Equipment

A total of three polymers are used in the fabrication of the sensors in this work. Two sensing polymers are synthesized, while the matrix polymer is used as is from the manufacturer. The materials used to form these polymers, along with their manufacturer and usage, are given below in Table 1.

**Table 1: MATERIALS USED IN SENSOR FABRICATION** 

Material	Manufacturer	Modification
Sylgard 184	Dow Silicones Corporation	Mixed to form cPDMS
SUPER C65 Conductive Carbon Black	MTI Corp	Mixed to form cPDMS
PEDOT:PSS (1.3% in H <sub>2</sub> O)	Sigma-Aldrich	Mixed to form PEDOT:PSS:TritonX
Triton X-100	Sigma-Aldrich	Mixed to form PEDOT:PSS:TritonX
Flex100	Monocure 3D	Used as is

Additionally, the equipment used is listed in Table 2 below.

 Table 2: EQUIPMENT USED

Equipment	Manufacturer	Usage
Photon DLP Printer	Anycubic	Sensor substrate fabrication
ARM-310 Mixer	Thinky	Sensing polymer fabrication
30M DIW Printer	Hyrel	Injecting sensing polymer
10 W UV LED Flood Lamp	QUANS	Curing polymers
Resistivity Four- Point Probe	Ossila	Resistivity characterization
TI 980 Nanoindenter	Bruker	Polymer mechanical characterization

LCR Meter	Hioki	Resistance Measurement
Criterion Universal Test Machine	MTS	Mechanical Deformation
VIC-3D DIC	Correlated Solutions	DIC Strain Mapping

#### 2.2 Sensor Fabrication

The printed sensor is fabricated utilizing primarily DLP to form the necessary sensing channels. A sensor optimized for detecting large amounts of deformation is designed and modeled. Several sensors are arranged onto a build plate, and since DLP printing time scales off of maximum printed part height (as opposed to certain AM techniques that scale off of total material printed, such as FDM), a total of 26 sensors are printed simultaneously [19-20]. After slicing the file using Chitubox, a file slicer for DLP printers, the sensor is printed with an Anycubic Photon DLP printer, utilizing Flex100, a UV curable polyacrylate. Manufacturing parameters are provided by the resin manufacturer and shown in Table 3.

**Table 3**: DLP MANUFACTURING PROPERTIES

Layer Height	50 μm
Bottom Layer Count	2
Exposure Time	11 s
Bottom Layer Exposure	60 s
Light Off Delay	11.5 s
Bottom Light Off Delay	0 s
Bottom Lift Distance	5 mm
Lifting Distance	5 mm
Bottom Lift Speed	65 mm/min
Lifting Speed	50 mm/min
Retract Speed	90 mm/min

After the part is fabricated, it is developed in a bath of isopropanol alcohol for 10 minutes, then is rinsed in fresh isopropanol alcohol, followed by water. After the wash cycles, the sensors are flood cured with a 400 nm 10 W ultraviolet (UV) lamp from a distance of 5 cm while remaining on the build plate for 5 minutes. Curing on the build plate reduces the warping that the sensors experience when being flood cured.

The sensors are filled with two different sensing materials: a PEDOT:PSS:TritonX mixture and a Carbon Black:PDMS mixture (1:6 weight ratio). The PEDOT:PSS:TritonX mixture (5:1 weight ratio, 6% wt. total) is an injectable polymer, while the cPDMS is a thick paste. The components for the PEDOT mixture are mixed with a Thinky ARM-310 mixer for twelve minutes (5 minutes at 1200 RPM, 2 minutes at 2000 RPM, and another 5 minutes at 1200 RPM) and degassed in a vacuum furnace. Samples to be filled with the PEDOT mixture are lifted from the build plate and laid onto a separate work surface, where the sensor channels are injected with the PEDOT:PSS:TritonX mixture via the use of a Hyrel Direct Ink Write printer, and wires

are inserted into the outermost wiring channels to acquire the resistance of the sensing material. For the cPDMS mixture, samples remained on the build plate, while the sensing material is applied directly to the channels. A scraper fills the channels and removes excess sensing material. These samples are then wired, removed from the build plate, and cured.

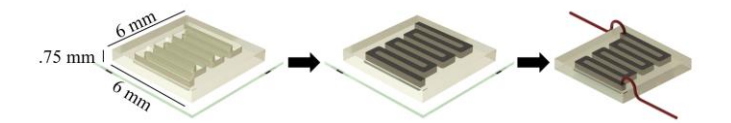


Figure 1: DETAILING THE FABRICATION PROCESS

After producing a full sensor, an embeddable testing substrate is manufactured utilizing a DLP printer. A dogbone test geometry based on an ASTM D638 dogbone pattern is used as the substrate base design. Inside of this dogbone, a section of space for the sensor is left in the design process. After slicing the file, the dogbone is printed with the Photon DLP printer, also utilizing the Flex100 as a substrate base to eliminate sensorsubstrate material mismatch. Once the print had progressed to the point where the space for the sensor is completely printed, (meaning the next printer layer would seal the opening) the completely wired sensor is fitted inside. As the sensor is inserted, the liquid resin vat fills any voids with liquid resin, completely encasing the sensor. The rest of the structure is then printed, with the sensor floating in an uncured resin pocket. After the completely filled internal seal is verified optically via microscopy (no bubbles or voids visible on any edges, and no liquid resin remains on the part exterior), the part is cured with the UV lamp for 15 minutes from a distance of 15 cm, which cures the liquid resin and sets the sensor inside the structure. After this, the sensor and substrate are completely set and fused into one functional test piece

# 2.3 Experimentation and Analysis

The electrochemical and mechanical properties of the sensing materials, as well as the Flex100 substrate resin, are tested to provide an understanding of the sensor characteristics. To test the materials' electrical properties, an Ossila 4 point probe is used to measure material resistivity. Sheets of the tested materials are cured and cut into 3 thin rectangles per material, which are approximately 13mm x 6mm, with a 30 micrometer sheet thickness. The results of these tests are shown below. Table 4 shows the results of the resistivity testing. No valid readings could be pulled from the Flex100, confirming it to be insular.

**Table 4:** RESISTIVITY OF PEDOT:PSS:TritonX AND CARBON-PDMS MIXTURES

	Primary Conductive Material	Resistivity $(n=3) (\Omega m)$
Carbon-PDMS	Carbon Black	$2.06E-1 \pm 2.42E-4$
PEDOT:PSS:TritonX	PEDOT	$2.72E-4 \pm 6.42E-7$

The sensing polymers are mechanically characterized using a Bruker TI 980 Nanoindenter system. The Young's Modulus of the Flex100 resin is found to be  $17.5 \pm 0.97$  MPa (n=3), and the hardness is found to be  $1.13 \pm 0.05$  MPa (n=3). To verify sensing polymer functionality, a simple validation test comparable to experimentation usually performed in literature [7,10,15] exploring new sensing polymers is performed to confirm the variation in resistance with deformation. Both of these sensing polymers have extensive literature [9,16,18,21-22] proving their viability in sensors. To replicate this, a cPDMS mixture is cured into a flat plate sensing element with an area of 7.62 cm by 2.54 cm. This plate is then wired on opposite ends, and mounted to an insular grip. The simple sensor is then deformed by bending to various angles, and the change in resistance due to the bending deformation is recorded. The plate is quickly deformed to a desired angle, and allowed to relax shortly after. Three distinct angles of 30°, 45°, and 60° are tested in one sweep. The results of these tests are shown in Figure 2. The figure shows a rapid response to strain with a jump in resistance, followed by a resistance drop to baseline over time. Different amounts of bending produce different increases in resistance, showing granularity beyond the detection of any deformation. Additional resistance sweeps provide a similar response. Thus, a distinct and varied change in resistance is shown for the simple sensing elements, verifying their strain sensing capabilities.

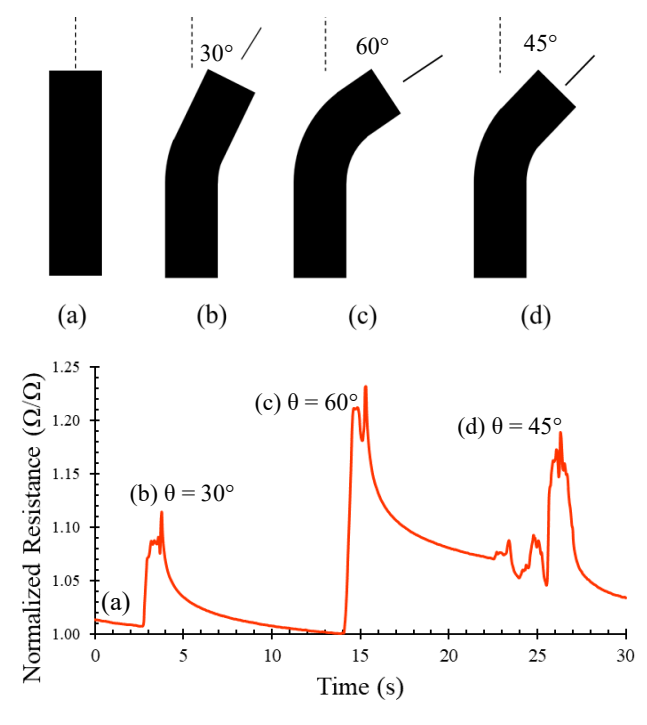


**FIGURE 2**: RESISTANCE CHANGE PLOTTED OVER TIME FOR BENDING DEFORMATION OF A SIMPLE SENSING PLATE

To verify the structural integrity of the substrate, tests without a sensor inside the DLP printed substrate are performed.

By virtue of the manufacturing process, the region of the dogbone intended for the sample is filled with liquid resin, which is fully cured in post-processing. If this section does not completely fuse, delamination and separation can occur, which would invalidate any sensor results. Three DLP dogbones are printed without a sensor inside, post-processed, and sprayed with a paint speckle for Digital Image Correlation (DIC) analysis utilizing VIC-3D, a fully featured DIC software that produces complete strain maps for detecting strain fields. An MTS (310 Criterion) is used to pull the DLP dogbones until failure at a testing rate of 5 mm/min. Results of the testing, including DIC analysis, are shown in Figures 3 and 4. Two different samples (a) and (b) are shown in Figure 4.

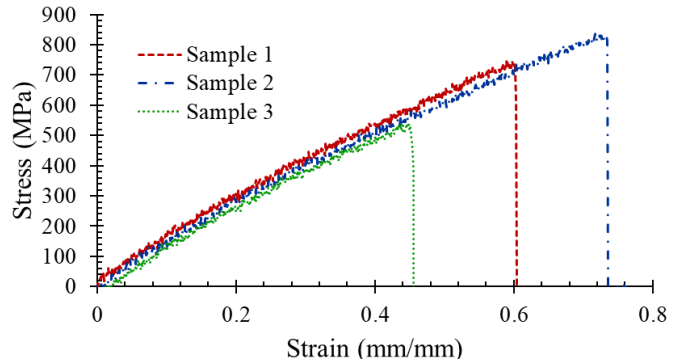


**FIGURE 3**: MECHANICAL TEST DATA FROM THE SOLID FILLED FLEX100 DOGBONE TESTS

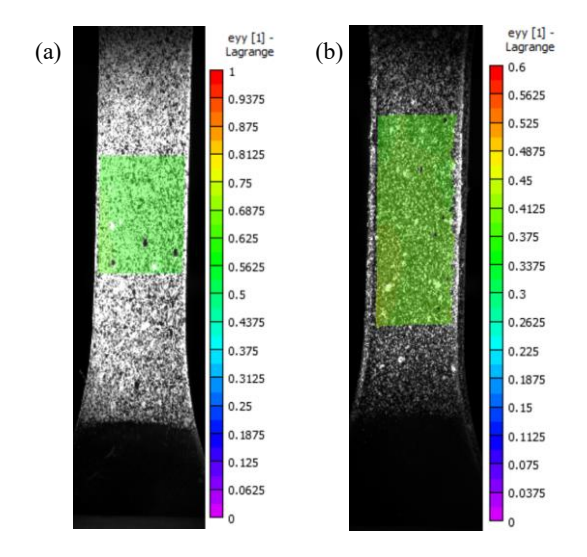


**FIGURE 4**: DIC MAPS OF THE TESTED POLYMER DOGBONES SHORTLY BEFORE FAILURE

The Flex100 dogbones all exhibited similar behavior, with a large amount of stretchability and similar failure methods. All dogbones tested failed from a Mode 1 fracture on the outer edge of the dogbone. The location of cracking varies with each dogbone, and did not correlate with sensor cavity location. The DIC mappings of the dogbones indicates no irregularities around the sensor cavity region, instead showing stress concentrations

only around the exterior crack locations. The lack of strain concentration in these regions indicates that no hairline crack or delamination is present, and that the polymer completely fused. After testing, the dogbones that did not fail at the sensor cavity are observed with microscopy to identify any potential delamination or separation. None of the failed samples show any visual signs of these defects, and the DIC maps show that the filled cavity behaves identically to a fully solidified part. The uniformity of the  $\epsilon$ -yy strain fields indicates even loading on the test samples throughout the testing.

After verifying the manufacturing technique integrity, a dogbone sample with a PEDOT:PSS:TritonX sensor inside is tested. The resistance of the sensing material is measured using a Hioki LCR meter, set to record resistance values at a rate of 20 Hz. The dogbone is strained until 10% deformation (5 mm total). Strain is calculated utilizing the DIC map reading in the gauge section of the dogbone. The DIC is set to measure the strain of just the sensor via a virtual extensometer.

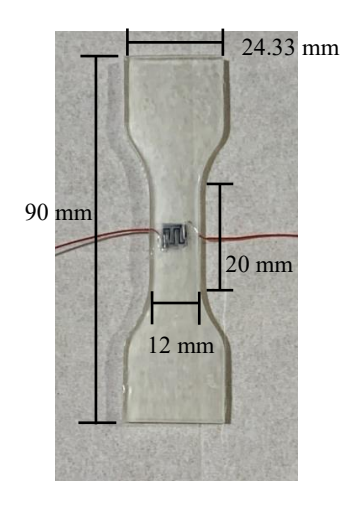


**FIGURE 5**: MANUFACTURED DOGBONE, WITH A WIRED SENSOR EMBEDDED IN THE CENTER.

#### 3. RESULTS AND DISCUSSION

The integrated sensing dogbone retains much of the flexibility and complaince of a completely solid polymer dogbone. No manufacturing defects are visible with microscopy. Unexpectedly, the process of embedding the sensor into the dogbone significantly increases the durability of the sensor in general, as the increased volume reduces the amount of concetrated stresses on the sample. Additionally, the extra casing prevents exterior elements from contacting the sensor, and completely insulates the sensor from external signals. However, care must be taken around the wiring in the edges of the dogbone. The presence of the wiring in the dogbone creates a material mismatch, and the wiring does not necessarily prefectly fuse with the Flex100 polymer. Thus, areas of weakness may be present in the immediate vicinity of the sensor.

The data from the mechanical testing is shown in Figure 6, plotting (a) Stress vs. Strain and (b) Resistance vs DIC Strain.

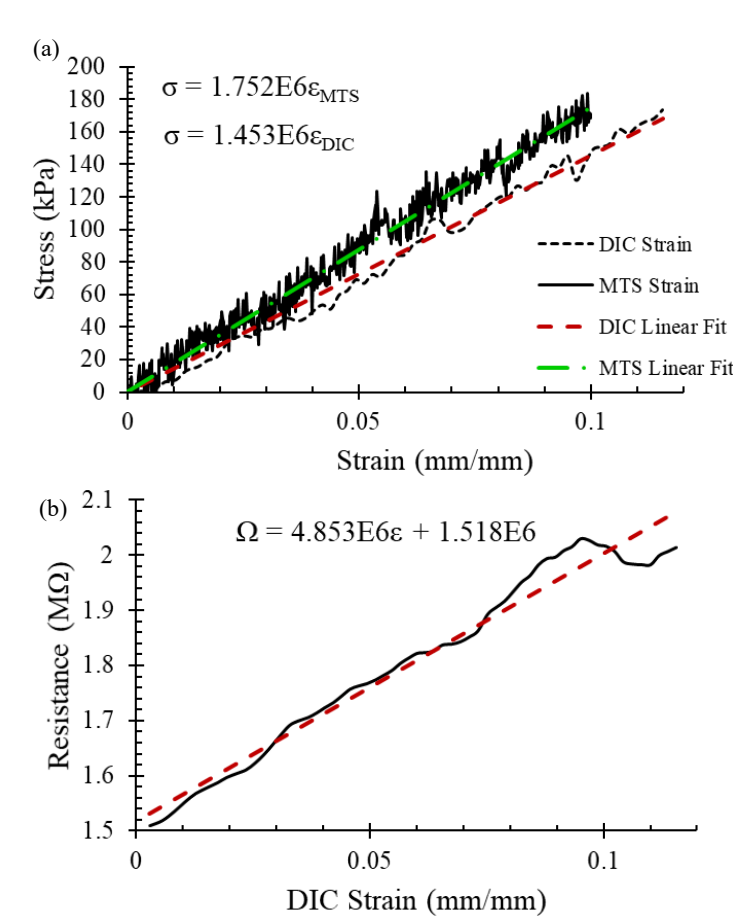


**FIGURE 6**: TESTING DATA OF THE SENSOR WITH AN EMBEDDED SENSOR

The results of this testing show a strong correlation between the mechanical strain and the resistance of the sensing element, confirming the efficacy of the sensor in a fabricated part. The sensor does not appear to negatively impact the mechanical response of the dogbone. The strain sensor shows strong linearity, with an  $R^2$  of .96 and a Gauge Factor of ~3.3. The sensor exhibits some minor variation toward the upper end of the loading, which could be a result of internal forces by the sensor installation and wiring.

The DIC mapping of the sensor indicates a region of lower strain around the sensor region in all stages of loading. This reduced region of strain evidences a locally stiffer region of the dogbone sample. Visual inspection of the region indicates that the senor wiring, which is much stiffer than the Flex100 polymer, creates regions of slightly less flexibility. Figure 7 shows the regions of decreased strain and increased stiffness are clearly visible around the area where the sensor wiring is present.

Overall, the sensor operates as intended, with strong sensing capabilities and easy integration. The embedding process of the sensor allows for the integration into any desired part, and the tunability of the sensor from manufacture allows for high sensor adaptability to a variety of structures and use cases.

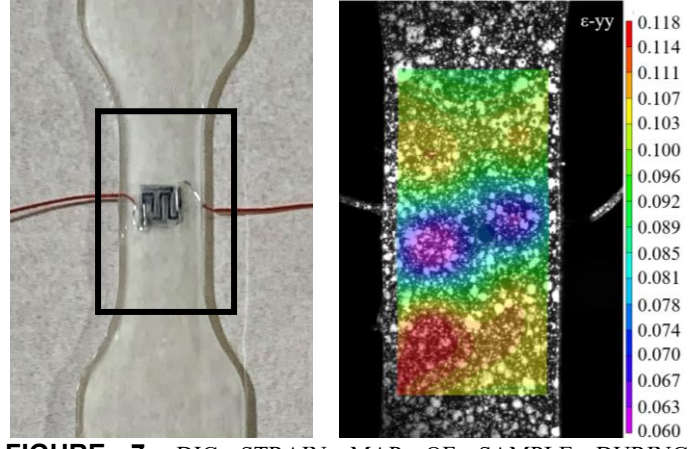


FIGURE 7: DIC STRAIN MAP OF SAMPLE DURING DEFORMATION

The manufacturing process detailed in this work is highly scalable, and can be optimized to print sensors at an exceptionally fast rate. While dependent on the desired sensor size, it is trivial to scale the slicing and printing to manufacture up to 360 sensors per print job. This print job only takes 10 minutes, and with a similar post processing time, sensors can be manufactured at over 1000 per hour. With better hardware (the Anycubic Photon is an entry level DLP printer), this amount could easily be doubled or tripled. As such, this work provides a framework for the rapid development and manufacture of large scale testing arrays.

The integration and refinement of new structural health monitoring technologies is a significantly more challenging task when working at a sub-macro scale implementation, whether that involves testing at the meso- to micro-scale, or increasing the resolution of a sensor at a macro-scale that involves aggregating multiple sensor sources. The dramatic reduction in size decreases the effective strength of the final product, and requires specialized tooling that is often incompatible with larger scales. Recent additive manufacturing advances have enabled the rapid progress into reliable and repeatable production of operational sensors at these difficult to work with scales.

#### 4. CONCLUSION

This work provides a simple proof-of-concept for a fully integrated sensor into any AM part. The flexibility afforded by the AM processes used allows for extreme adaptability. The integrated sensors can easily be configured for other sensing cases, such as pressure or temperature, and the substrate shape can be adapted to fit complex geometry with ease. Future work will explore this customization for practical applications requiring customizable micro-scale sensing.

## **REFERENCES**

- [1] Moore, Christopher L. "Gossamer spacecraft technology for space solar power systems." In 2001 IEEE Aerospace Conference Proceedings (Cat. No. 01TH8542), vol. 7, pp. 7-3589. IEEE, 2001.
- [2] Sodano, Henry A., Gyuhae Park, and Daniel J. Inman. "Multiple sensors and actuators for vibration suppression of an inflated torus." *Journal of spacecraft and rockets* 42, no. 2 (2005): 370-373.
- [3] Lin, Yirong, and Henry A. Sodano. "Fabrication and electromechanical characterization of a piezoelectric structural fiber for multifunctional composites." *Advanced Functional Materials* 19, no. 4 (2009): 592-598.
- [4] Polese, Davide, Luca Maiolo, Luca Pazzini, Guglielmo Fortunato, Alessio Mattoccia, and Pier Gianni Medaglia. "Wireless sensor networks and flexible electronics as innovative solution for smart greenhouse monitoring in long-term space missions." In 2019 IEEE 5th International Workshop on Metrology for AeroSpace (MetroAeroSpace), pp. 223-227. IEEE, 2019.
- [5] Li, Qi, Lei Chen, Matthew R. Gadinski, Shihai Zhang, Guangzu Zhang, Haoyu U. Li, Elissei Iagodkine et al. "Flexible high-temperature dielectric materials from polymer nanocomposites." *Nature* 523, no. 7562 (2015): 576-579.
- [6] Kao, Hsuan-Ling, Cheng-Lin Cho, Li-Chun Chang, Chun-Bing Chen, Wen-Hung Chung, and Yun-Chen Tsai. "A fully inkjet-printed strain sensor based on carbon nanotubes." *Coatings* 10, no. 8 (2020): 792.
- [7] Lu, Nanshu, Chi Lu, Shixuan Yang, and John Rogers. "Highly sensitive skin-mountable strain gauges based entirely on elastomers." Advanced Functional Materials 22, no. 19 (2012): 4044-4050.
- [8] Srinivasaraghavan Govindarajan, Rishikesh, Eduardo Rojas-Nastrucci, and Daewon Kim. "Surface Acoustic Wave-Based Flexible Piezocomposite Strain Sensor." *Crystals* 11, no. 12 (2021): 1576.
- [9] Tevi, Tete, Shantonio W. Saint Birch, Sylvia W. Thomas, and Arash Takshi. "Effect of Triton X-100 on the double layer capacitance and conductivity of poly (3, 4-ethylenedioxythiophene): poly (styrenesulfonate)(PEDOT: PSS) films." Synthetic metals 191 (2014): 59-65.
- [10] Kao, Hsuan-Ling, Cheng-Lin Cho, Li-Chun Chang, Chun-Bing Chen, Wen-Hung Chung, and Yun-Chen Tsai. "A fully inkjet-printed strain sensor based on carbon nanotubes." *Coatings* 10, no. 8 (2020): 792.
- [11] Wan, Shu, Zhihong Zhu, Kuibo Yin, Shi Su, Hengchang Bi, Tao Xu, Hongtao Zhang, Zhihui Shi, Longbing He, and Litao Sun. "A Highly Skin-Conformal and Biodegradable Graphene-Based Strain Sensor." *Small Methods* 2, no. 10 (2018): 1700374.
- [12] Srinivasaraghavan Govindarajan, Rishikesh, Taylor Stark, Stanislav Sikulskyi, Foram Madiyar, and Daewon Kim. "Piezoelectric strain sensor through reverse replication

- based on two-photon polymerization." In *Proc. of SPIE Vol.*, vol. 12046, pp. 1204611-1.
- [13] Peng, Jun, Shuhai Jia, Yiming Jin, Shouping Xu, and Zaide Xu. "Design and investigation of a sensitivity-enhanced fiber Bragg grating sensor for micro-strain measurement." Sensors and Actuators A: Physical 285 (2019): 437-447.
- [14] Assaifan, Abdulaziz K., Jonathan S. Lloyd, Siamak Samavat, Davide Deganello, Richard J. Stanton, and Kar Seng Teng. "Nanotextured surface on flexographic printed ZnO thin films for low-cost non-faradaic biosensors." ACS Applied Materials & Interfaces 8, no. 49 (2016): 33802-33810.
- [15] Ye, Fengming, Meng Li, Dingning Ke, Liping Wang, and Yi Lu. "Ultrafast Self-Healing and Injectable Conductive Hydrogel for Strain and Pressure Sensors." *Advanced Materials Technologies* 4, no. 9 (2019): 1900346.
- [16] Karuthedath, Cyril Baby, Ubaidul Fikri, Friederike Ruf, and Norbert Schwesinger. "Characterization of carbon black filled PDMS-composite membranes for sensor applications." In Key engineering materials, vol. 753, pp. 18-27. Trans Tech Publications Ltd, 2017.
- [17] Zhao, Jing, Guole Wang, Rong Yang, Xiaobo Lu, Meng Cheng, Congli He, Guibai Xie, Jianling Meng, Dongxia Shi, and Guangyu Zhang. "Tunable piezoresistivity of nanographene films for strain sensing." *ACS nano* 9, no. 2 (2015): 1622-1629.
- [18] Vuorinen, Tiina, Juha Niittynen, Timo Kankkunen, Thomas M. Kraft, and Matti Mäntysalo. "Inkjet-printed graphene/PEDOT: PSS temperature sensors on a skin-conformable polyurethane substrate." Scientific reports 6, no. 1 (2016): 1-8.
- [19] ASTM. "Standard terminology for additive manufacturing." *ASTM 52900-15* (2015).
- [20] Masiuchok, Olha, Maksym Iurzhenko, Valeriy Demchenko, and Mykola Korab. "Comparative analysis of the quality of plastic products formed by DLP and FDM 3D printing technologies." Вісник Тернопільського національного технічного університету 98, по. 2 (2020): 40-48.
- [21] Wang, Yi-Fei, Tomohito Sekine, Yasunori Takeda, Koji Yokosawa, Hiroyuki Matsui, Daisuke Kumaki, Takeo Shiba, Takao Nishikawa, and Shizuo Tokito. "Fully printed PEDOT: PSS-based temperature sensor with high humidity stability for wireless healthcare monitoring." Scientific reports 10, no. 1 (2020): 1-8.
- [22] Niu, X. Z., S. L. Peng, L. Y. Liu, W. J. Wen, and Ping Sheng. "Characterizing and patterning of PDMS-based conducting composites." Advanced Materials 19, no. 18 (2007): 2682-2686.